



## Inflammasome Reporter Cells

All you have to do is ASC

In vivoGen



### Stalk Region of $\beta$ -Chain Enhances the Coreceptor Function of CD8

Jenny S. Wong, Xiaosong Wang, Torsten Witte, Linghu Nie, Nicolas Carvou, Petra Kern and Hsiu-Ching Chang

This information is current as of February 5, 2018.

*J Immunol* 2003; 171:867-874; ;  
doi: 10.4049/jimmunol.171.2.867  
<http://www.jimmunol.org/content/171/2/867>

#### Why *The JI*?

- **Rapid Reviews! 30 days\*** from submission to initial decision
- **No Triage!** Every submission reviewed by practicing scientists
- **Speedy Publication!** 4 weeks from acceptance to publication

*\*average*

**References** This article **cites 48 articles**, 18 of which you can access for free at:  
<http://www.jimmunol.org/content/171/2/867.full#ref-list-1>

**Subscription** Information about subscribing to *The Journal of Immunology* is online at:  
<http://jimmunol.org/subscription>

**Permissions** Submit copyright permission requests at:  
<http://www.aai.org/About/Publications/JI/copyright.html>

**Email Alerts** Receive free email-alerts when new articles cite this article. Sign up at:  
<http://jimmunol.org/alerts>



# Stalk Region of $\beta$ -Chain Enhances the Coreceptor Function of CD8<sup>1</sup>

Jenny S. Wong, Xiaosong Wang, Torsten Witte, Linghu Nie, Nicolas Carvou, Petra Kern, and Hsiu-Ching Chang<sup>2</sup>

CD8 glycoproteins are expressed as either  $\alpha\alpha$  homodimers or  $\alpha\beta$  heterodimers on the surface of T cells. CD8 $\alpha\beta$  is a more efficient coreceptor than the CD8 $\alpha\alpha$  for peptide Ag recognition by TCR. Each CD8 subunit is composed of four structural domains, namely, Ig-like domain, stalk region, transmembrane region, and cytoplasmic domain. In an attempt to understand why CD8 $\alpha\beta$  is a better coreceptor than CD8 $\alpha\alpha$ , we engineered, expressed, and functionally tested a chimeric CD8 $\alpha$  protein whose stalk region is replaced with that of CD8 $\beta$ . We found that the  $\beta$  stalk region enhances the coreceptor function of chimeric CD8 $\alpha\alpha$  to a level similar to that of CD8 $\alpha\beta$ . Surprisingly, the  $\beta$  stalk region also restored functional activity to an inactive CD8 $\alpha$  variant, carrying an Ala mutation at Arg<sup>8</sup> (R8A), to a level similar to that of wild-type CD8 $\alpha\beta$ . Using the R8A variant of CD8 $\alpha$ , a panel of anti-CD8 $\alpha$  Abs, and three MHC class I (MHCI) variants differing in key residues known to be involved in CD8 $\alpha$  interaction, we show that the introduction of the CD8 $\beta$  stalk leads to a different topology of the CD8 $\alpha$ -MHCI complex without altering the overall structure of the Ig-like domain of CD8 $\alpha$  or causing the MHCI to employ different residues to interact with the CD8 $\alpha$  Ig domain. Our results show that the stalk region of CD8 $\beta$  is capable of fine-tuning the coreceptor function of CD8 proteins as a coreceptor, possibly due to its distinct protein structure, smaller physical size and the unique glycan adducts associated with this region. *The Journal of Immunology*, 2003, 171: 867–874.

CD8 is a membrane-anchored glycoprotein that functions as a coreceptor for Ag recognition of the peptide/MHC class I (MHCI)<sup>3</sup> complexes by TCRs (1–4) and plays an important role in T cell development in the thymus and T cell activation in the periphery (5–8). Functional CD8 is a dimeric protein made of either two  $\alpha$ -chains (CD8 $\alpha\alpha$ ) or an  $\alpha$ -chain and a  $\beta$ -chain (CD8 $\alpha\beta$ ) (9–11), and the surface expression of the  $\beta$ -chain requires its association with the coexpressed  $\alpha$ -chain to form the CD8 $\alpha\beta$  heterodimer (12, 13). Importantly, CD8 $\alpha\alpha$  and CD8 $\alpha\beta$  are differentially expressed on a variety of lymphocytes. CD8 $\alpha\beta$  is expressed predominantly on the surface of  $\alpha\beta$ TCR<sup>+</sup>T cells and thymocytes (14–17), and CD8 $\alpha\alpha$  on a subset of  $\alpha\beta$ TCR<sup>+</sup>,  $\gamma\delta$ TCR<sup>+</sup> intestinal intraepithelial lymphocytes, NK cells, dendritic cells, and a small fraction of CD4<sup>+</sup> T cells (17–19). The differential distributions of CD8 $\alpha\alpha$  and CD8 $\alpha\beta$  suggest that these two forms of CD8 are likely to mediate distinct functions.

Recent reports showed that CD8 $\alpha\beta$  is more effective than CD8 $\alpha\alpha$  to facilitate recognition of the same peptide Ag by TCR (20, 21). It appears that heterodimerization with the  $\beta$ -chain per se is sufficient to enhance the kinase activity of the CD8 $\alpha$ -chain-associated *lck* (22). The cytoplasmic domain of CD8 $\beta$  has been implicated in this enhancement of coreceptor function, as palmy-

tylation of a Cys residue in this region during T cell activation can effectively facilitate the partition of TCR/CD8 $\alpha\beta$  complexes into lipid rafts (23). On the other hand, we showed previously that the extracellular domain of the CD8 $\beta$ -chain alone is also capable of enhancing the coreceptor function of the CD8 $\alpha\beta$  molecule (20). This is collaborated with earlier observations that the extracellular domain of CD8 $\beta$  is responsible for enhanced coreceptor functions for recognition of allogeneic Ag (24, 25) and for a better interaction with MHC tetramers (26, 27).

CD8 $\alpha$  and  $\beta$  subunits have similar structural motifs, including an Ig-like domain, a stalk region of 30–40 aa, a transmembrane region, and a short cytoplasmic domain of ~20 aa (reviewed in Ref. 28). CD8 $\alpha$ - and  $\beta$ -chains have two and one *N*-linked glycosylation sites, respectively, in the Ig-like domains where they share <20% identity in their amino acid sequences (12–15, 26). The CD8 $\beta$  stalk region is 10–13 aa shorter than the CD8 $\alpha$  stalk and is highly glycosylated with *O*-linked carbohydrates. These carbohydrates on the  $\beta$ , but not the  $\alpha$ , stalk region appear to be quite heterogeneous due to complex sialylations, which are differentially regulated during the developmental stages of thymocytes (27, 29–31) and upon activation of T cells (32). Indeed, glycan adducts have been shown to play regulatory roles in the functions of glycoproteins and in immune responses (reviewed in Ref. 33), and glycans proximal to transmembrane domains can affect the orientation of adjacent motifs (34). The unique biochemical properties of the CD8 $\beta$ -chain stalk region make it a plausible candidate for modulating the coreceptor function.

To determine whether the  $\beta$  stalk region is responsible for the enhanced Ag recognition activity of CD8 $\alpha\beta$ , we created a chimeric CD8 $\alpha$  protein whose stalk region is replaced by the  $\beta$  stalk region and tested its coreceptor function in a T cell hybridoma system. Our data indicate that the introduction of the  $\beta$  stalk region alters the overall topology of CD8 $\alpha$ -MHCI complexes and drastically enhances the coreceptor function of chimeric CD8 $\alpha\alpha$  homodimers.

Dana-Farber Cancer Institute, Department of Cancer Immunology and AIDS, Harvard Medical School, Boston, MA 02115

Received for publication February 7, 2003. Accepted for publication May 12, 2003.

The costs of publication of this article were defrayed in part by the payment of page charges. This article must therefore be hereby marked *advertisement* in accordance with 18 U.S.C. Section 1734 solely to indicate this fact.

<sup>1</sup> This work was supported by National Institutes of Health Grant AI45789 (to H.-C.C.). J.W. is a recipient of the Friends Grant from Dana-Farber Cancer Institute.

<sup>2</sup> Address correspondence and reprint requests to Dr. Hsiu-Ching Chang, Dana-Farber Cancer Institute, Harvard Medical School, 44 Binney Street, Boston, MA 02115. E-mail address: hsiu-ching\_chang@dfci.harvard.edu

<sup>3</sup> Abbreviations used in this paper: MHCI, MHC class I;  $\beta_2$ M,  $\beta_2$ -microglobulin; TM, transmembrane segment; VSV, vesicular stomatitis virus; wt, wild type.

## Materials and Methods

### Monoclonal Abs

Anti-H-2K<sup>b</sup>-specific mAbs 5F1-2-14 (5F1), EH144, Y3, and 28.13.3 were used to monitor the expression level of H-2K<sup>b</sup> on the R8 APCs as previously described (35). Anti-mouse CD8 $\alpha$  mAbs 53.6.72, 19/178, H59, YTS105, and YTS169 as well as anti-mouse CD8 $\beta$  mAb YTS156.7 were used to monitor the expression of these CD8 proteins. Anti-mouse TCR V $\beta$ 5.2 mAb MR9.4 were used to verify the surface expression of TCR (36). Anti-mouse CD8 $\alpha$  mAb 53.6.72 or anti-mouse CD8 $\beta$  mAb YTS156.7 was used for immunoprecipitation of each CD8 subunit. Anti-mouse CD3 $\epsilon$  145.2C11 was used to stimulate the N15 hybridoma cells as a positive control for IL-2 production (37).

### Flow cytometric analysis

Indirect flow cytometric analysis was performed on the parental N15CD8<sup>-</sup> cells (negative for CD8 expression), and N15 cells expressing CD8 variants for the surface expression of TCR, CD8 $\alpha$ , and CD8 $\beta$  molecules by incubating each cell line with a specific Ab, followed by a secondary Ab (anti-murine or anti-rat) conjugated with FITC (Caltag, San Francisco, CA). A minimum of 5000 cells were analyzed by FACS for each sample.

### Mutant H-2K<sup>b</sup> APC

APC R8 is a pre-B lymphoma cell line that was transformed with Abelson leukemia virus and was used to present the VSV8 peptide in the context of wild-type H-2K<sup>b</sup>. R8.161 is a cell line derived from the parental R8 line that lacks the expression of H-2K<sup>b</sup> (35); it was transfected with cDNAs encoding H-2K<sup>b</sup> variants to generate the corresponding APCs. To generate alanine substitution mutations in H-2K<sup>b</sup>, the H-2K<sup>b</sup> cDNA was used as a template for a PCR-based mutagenesis. A single alanine mutation was introduced in the cDNA of H-2K<sup>b</sup> corresponding to residues Lys<sup>198</sup> (K198), Gln<sup>226</sup> (Q226), or Asp<sup>227</sup> (D227). Mutated cDNAs were ligated into the pCRII vector (Invitrogen, San Diego, CA) for sequence confirmation. The verified constructs were subcloned into the pSH-xs expression vector, which carries the hygromycin resistance gene (37). The individual cDNA construct was then transfected into the R8.161 line to generate H-2K<sup>b</sup> mutant lines, R8.K198A, R8.Q226A, or R8.D227A, as previously described (35). These transfectants were sorted by FACS and selected for clones whose H-2K<sup>b</sup> expression levels are similar to that of parental R8 cells.

### CD8 $\alpha$ constructs

To generate the CD8 $\alpha$ <sup>R8A</sup> mutant, mCD8 $\alpha$  was subjected to mutagenesis using a PCR method as described above. The cDNAs encoding the mutated CD8 $\alpha$  (CD8 $\alpha$ <sup>R8A</sup>) were then subcloned into pSH-xs. The chimeric CD8 $\alpha$  (CD8 $\alpha$ - $\beta$ - $\alpha$ ) construct was generated by ligation of three cDNA fragments: the *Xba*I-*Bsr*I fragment encoding the Ig-like domain of CD8 $\alpha$ , the *Bsr*I-*Nsp*I fragment encoding the stalk region of the CD8 $\beta$ , and the *Nsp*I-*Sac*I fragment encoding the transmembrane segment (TM) and the cytoplasmic domain of CD8 $\alpha$ . The *Xba*I-*Bsr*I fragment and *Bsr*I-*Nsp*I fragment were obtained by restricted digestion of the cDNA construct encoding the wild-type CD8 $\alpha$ . The *Bsr*I-*Nsp*I fragment was obtained by PCR from the cDNA construct encoding the wild-type CD8 $\beta$  using a 5' primer, which contains the *Bsr*I site encoding the very C terminus of the CD8 $\alpha$  Ig-like domain fused with a small segment of DNA encoding the N-terminal portion of the CD8 $\beta$  stalk region, and a 3' primer, which contains a small DNA segment encoding the C-terminal portion of the CD8 $\beta$  stalk region, followed by the *Nsp*I site-containing segment encoding for the N-terminal portion of the TM domain of CD8 $\alpha$ . The cDNA was sequence-verified and subcloned into the pSH-xs vector. The construct encoding the chimeric CD8 $\alpha$ <sup>R8A</sup> (CD8 $\alpha$ <sup>R8A</sup>- $\beta$ - $\alpha$ ) was similarly generated, except that the *Xba*I-*Bsr*I fragment encoding the Ig-like region was released by restriction digestion from the cDNA construct of CD8 $\alpha$ <sup>R8A</sup>.

### N15 transfectants expressing CD8 $\alpha$ variants

To generate the cell line expressing homodimeric CD8 $\alpha$ <sup>R8A</sup>- $\alpha$ <sup>R8A</sup>, ~10<sup>7</sup> parental N15CD8<sup>-</sup> cells were electroporated with 10  $\mu$ g of *Sa*I-linearized pSH-CD8 $\alpha$ <sup>R8A</sup> at 250 V and 800  $\mu$ F using a cell electroporator (Life Technologies, Gaithersburg, MD). After 48 h the cells were plated in complete RPMI 1640 medium containing 2 mg/ml of hygromycin at a density of 2  $\times$  10<sup>4</sup> cells/well in 24-well plates and cultured for 2 wk. Hygromycin-resistant clones were analyzed for CD8 $\alpha$  expression by FACS. A minimum of 20 positive clones were pooled and sorted for similar levels of CD8 expression. To generate the cell lines expressing the CD8 $\alpha$ <sup>R8A</sup> $\beta$  heterodimer, the same method was used, except the mutant CD8 $\alpha$ <sup>R8A</sup> and wild-type

CD8 $\beta$  were cotransfected into the parental N15CD8<sup>-</sup> cells. The resulting transfectants were tested for the cell surface expression of TCR, CD8 $\alpha$ , and CD8 $\beta$  by FACS. The coreceptor functions of these cell lines were examined by IL-2 production triggered by R8 APCs loaded with various concentrations of VSV8 peptide. The expression of functional TCR in each N15 transfectant was positively verified by IL-2 production induced by cross-linking of TCR with an anti-CD3 $\epsilon$  Ab, 2C11.

### IL-2 production assay and inhibition of coreceptor function by anti-CD8 $\alpha$ mAb Abs

The IL-2 production of the CD8-expressing N15 transfectants was quantified using the MTT assay (37). The parental R8 APC or mutant APCs expressing H-2K<sup>b</sup> variants R8.K198A, R8.Q226A, or R8.D227A were irradiated (3300 rad) and loaded with VSV8 peptide at concentrations ranging from 10<sup>-9</sup> to 10<sup>-4</sup> M at 37°C for 2 h. Approximately 1  $\times$  10<sup>5</sup> transfectants were then incubated with an equal number of APCs in a total volume of 200  $\mu$ l of complete RPMI supplemented with 10 ng/ml of PMA in 96-well plates for 24 h. Supernatants were harvested and stored at -70°C. CTLL-20 cells, an IL-2-dependent cell line, were incubated with serially diluted supernatant in 96-well plates (10<sup>4</sup> cells/well) for 48 h. The MTT substrate (3-[4,5-dimethylthiazol-2-yl]-5-diphenyltetrazolium bromide; Sigma-Aldrich, St. Louis) was added 4 h before harvesting by dissolving cells in SDS/isopropanol/HCl. The solubilized MTT product was measured at 570 nm using the SpectraMax 250 spectrophotometer (Molecular Devices, Sunnyvale, CA). The IL-2 concentrations in the supernatants were determined based on the standard curve generated by purified recombinant human IL-2 (Chiron, Emeryville, CA).

Inhibition of coreceptor function by anti-CD8 $\alpha$  mAbs was analyzed similarly to the IL-2 production assay, except that 10  $\mu$ g/ml of affinity-purified anti-CD8 $\alpha$  mAb, 53.6.72, YTS169, or YTS169 Fab in RPMI medium was added to 1  $\times$  10<sup>6</sup> N15 cells expressing CD8 $\alpha$  variants for 30 min before incubation with peptide-loaded APCs.

### SDS-PAGE analysis of CD8 proteins

The cell surface CD8 proteins were analyzed by immunoprecipitation of lysates prepared from the CD8 transfectants (20). Briefly, ~10<sup>7</sup> cells were surface biotinylated and solubilized by lysis buffer containing TBS (10 mM Tris and 150 mM NaCl, pH 7.6), 1% Triton X-100, 1% aprotinin, 1 mM PMSF, 2 mM EDTA, and 5  $\mu$ g/ml leupeptin. Postnuclear supernatants were precleared and immunoprecipitated using anti-CD8 $\alpha$  mAb, 53.6.72; anti-CD8 $\beta$  mAb, YTS156; or control mAb, 2H11, prebound to  $\gamma$  Bind Plus beads (Amersham Pharmacia Biotech, Arlington Heights, IL). After washing the beads four times with lysis buffer, beads were treated with Laemmli sample buffer, boiled, and resolved by a 12.5% SDS-PAGE under reducing conditions. Proteins were blotted onto nitrocellulose membranes and probed with HRP-conjugated streptavidin, followed by visualization using the ECL substrates (Amersham Pharmacia Biotech).

## Results

### Comparison of the stalk regions of CD8 $\alpha$ and CD8 $\beta$

Both CD8 $\alpha$  and CD8 $\beta$  contain a stalk region that is directly adjacent to the Ig-like domain and may therefore play a role in mediating CD8-MHCI interaction. To investigate the role(s) of the stalk region, we compared the polypeptide sequences of both CD8 $\alpha$  and CD8 $\beta$  stalk regions of murine, rat, and human proteins. In Fig. 1A, polypeptide sequences are aligned by a pair of conserved cysteine residues. The Cys<sup>151</sup> and Cys<sup>166</sup> of the murine CD8 $\alpha$  are aligned with Cys<sup>137</sup> and Cys<sup>150</sup> of the murine CD8 $\beta$ . This alignment reveals that for the region before the first cysteine residue (Asn<sup>123</sup> to Asp<sup>150</sup> in murine CD8 $\alpha$  and Asp<sup>116</sup> to Gln<sup>136</sup> in murine CD8 $\beta$ ) CD8 $\alpha$  is less conserved than CD8 $\beta$ , with 28% (8 of 28) and 66% (14 of 21) identity, respectively. For the region between the aligned cysteine residues, CD8 $\alpha$  and CD8 $\beta$  have a similar degree of conservation between species, but have no obvious homology to each other within the same species. Overall, compared with CD8 $\alpha$ , CD8 $\beta$  has a shorter (35 vs 44 residues for murine proteins) and more conserved (66 vs 28%, among murine, rat, and human proteins) stalk region. Differences revealed by this

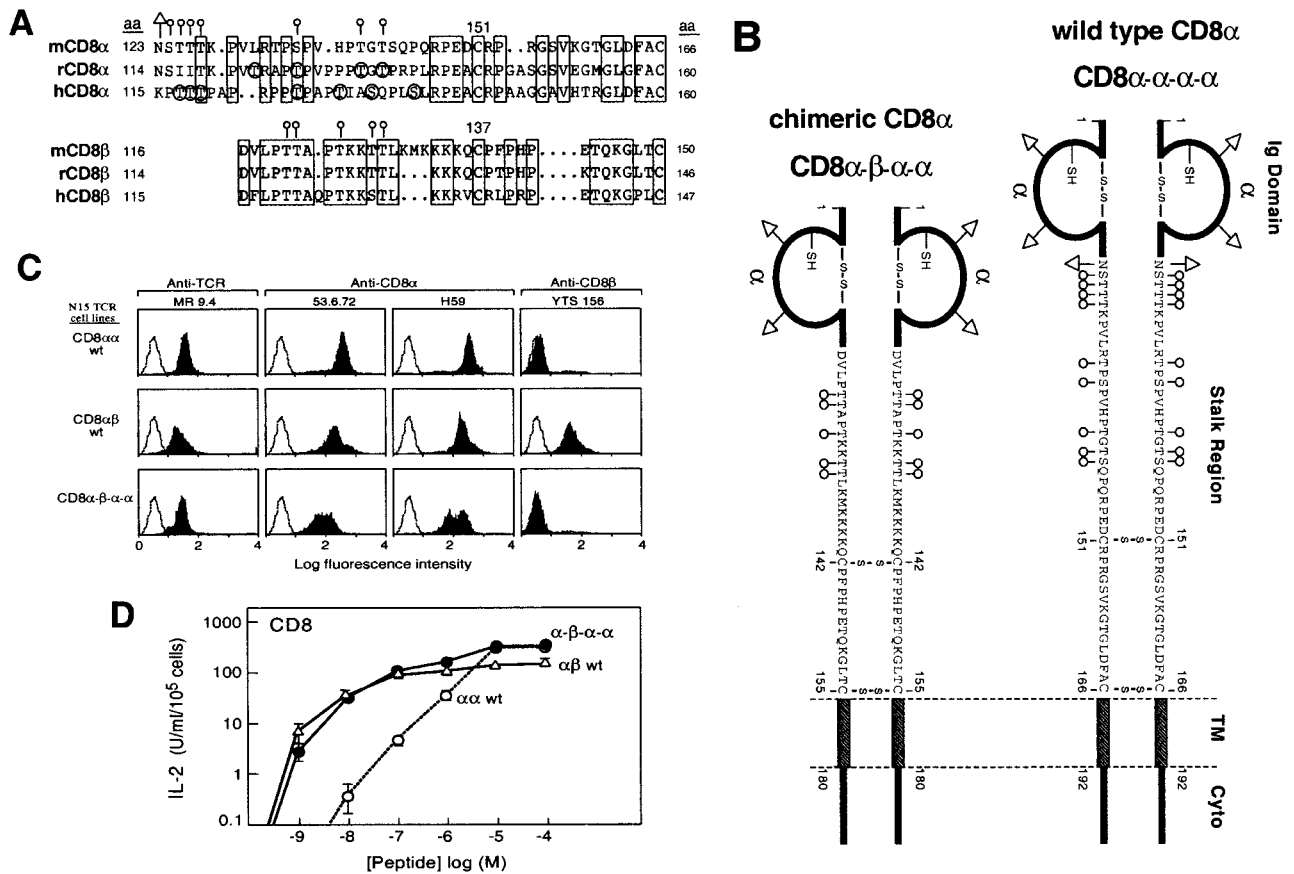


**FIGURE 1.** The  $\beta$  stalk region enhances the Ag sensitivity of the CD8 $\alpha$  coreceptor. **A**, Comparison of the protein sequences of the stalk regions of mouse (m), rat (r), and human (h) CD8 $\alpha$  and  $\beta$ . The alignment is based on the conserved cysteine residues amino terminal to the TM domains of CD8 $\alpha$  and  $\beta$ , with identical residues among the species boxed. Note the remarkable conservation of the amino acids between 116–150 (m) of the  $\beta$ -chain, which contains five conserved potential *O*-linked glycosylation sites (open circle lollipop). Known sites of *O*-linked glycosylation in rat CD8 $\alpha$  and proposed glycosylation in human CD8 $\alpha$  are circled (45, 46). A potential *N*-linked glycosylation site in murine CD8 $\alpha$  is marked as a triangle lollipop, and a potential *O*-linked glycosylation site is marked as open circle lollipop. Note that the potential glycosylation sites of CD8 $\alpha$  among the species are not well conserved. No sequence homology between the CD8 $\alpha$  and  $\beta$  stalks is evident in this comparison. **B**, Schematic representation of wild-type CD8 $\alpha$  and chimeric CD8 $\alpha$ . Wild-type CD8 $\alpha$  is composed of two  $\alpha$  subunits held together by two disulfide bonds at the stalk regions. Each  $\alpha$  subunit includes four domains: one Ig-like domain (aa 1–122) containing two *N*-linked glycosylation sites (open triangle lollipop), one 44-residue (aa 123–166) long stalk region containing one potential *N*-linked glycosylation site and multiple *O*-linked sites, one TM (aa 167–192), and one cytoplasmic tail (Cyto; aa 193–220) containing an *lck*-binding motif. The chimeric CD8 $\alpha$ , ( $\alpha$ - $\beta$ - $\alpha$ - $\alpha$ )<sub>2</sub>, is phenotypically a CD8 $\alpha$  homodimer, but has a  $\beta$  stalk region instead of an  $\alpha$  stalk region. The most notable difference is that one potential *N*-linked and a cluster of *O*-linked glycosylation sites are missing immediately adjacent to the Ig-like domain. **C**, FACS analysis of the N15 CD8 transfectants. The surface expression of TCR, CD8 $\alpha$ , and CD8 $\beta$  epitopes on the transfectants was detected by indirect fluorescence staining with specific mAbs, and species-specific secondary Abs. The filled curve represents specific staining with mAb, and the open curve corresponds to background staining (FITC-labeled secondary Ab alone). Histograms were compiled from a minimum of 5000 cells. In these cells only CD8 $\alpha$ β wild type expresses the CD8 $\beta$  Ig domain on the cell surface. **D**, IL-2 production assay of the transfectants expressing CD8 variants. CD8 $\alpha$  transfectants were activated with H-2K<sup>b</sup> R8 APC pulsed with 10<sup>-9</sup>–10<sup>-4</sup> M VSV8 peptide. IL-2 production curves of the transfectants are shown as an open circle for CD8 $\alpha$ α-wt, a triangle for CD8 $\alpha$ β-wt, and a filled circle for the chimeric CD8 $\alpha$ .

alignment suggest that the stalk region of CD8 $\beta$  may have a role distinct from the stalk region of CD8 $\alpha$ .

#### Stalk region of CD8 $\beta$ subunit enhances the coreceptor function of CD8 $\alpha$

To examine the role of the CD8 $\beta$  stalk, we created a chimeric CD8 $\alpha$  (CD8 $\alpha$ - $\beta$ - $\alpha$ - $\alpha$ ) subunit by replacing the stalk region of wild-type CD8 $\alpha$  (CD8 $\alpha$ - $\alpha$ - $\alpha$ - $\alpha$ ) with the stalk region of CD8 $\beta$  (Fig. 1B). The chimeric CD8 $\alpha$  is now nine residues shorter than the wild-type CD8 $\alpha$  and lacks the *N*-linked and a cluster of *O*-linked carbohydrates present in the wild-type protein directly following the Ig-like domain. The chimeric CD8 $\alpha$  was then transfected into a T cell hybridoma N15TCRCD8<sup>-</sup> cell line whose TCR is specific for the VSV8 peptide Ag (vesicular stomatitis virus nucleocapsid protein residues 52–59, RGYVYQGL) in the context of H-2 K<sup>b</sup>, but lacks the expression of

the CD8 protein (37). As shown in Fig. 1C, the chimeric CD8 $\alpha$  is able to express, on the cell surface, a comparable level of N15TCR as detected by MR 9.4, and CD8 $\alpha$  molecules, detected by 53.6.72, and H59 Ab to the CD8 $\alpha$ , or CD8 $\alpha$ β wild-type cell lines. Only CD8 $\alpha$ β wild type has detectable CD8 $\beta$  on the surface, as detected by CD8 $\beta$  Ig domain-specific Ab, YTS156 (36). With the introduction of the chimeric CD8 $\alpha$  coreceptor, this cell can be triggered by VSV8 peptide Ag to produce IL-2 (Fig. 1D). Interestingly, at concentrations of peptide Ag <10<sup>-6</sup> M, the chimeric CD8 $\alpha$ -expressing cells are 40–100 times more sensitive than the wild-type CD8 $\alpha$ -expressing cells, while at higher Ag concentrations such a difference was no longer observed. The IL-2 production curve of chimeric CD8 $\alpha$  is almost identical with that of CD8 $\alpha$ β wild type (Fig. 1D). Thus, the CD8 $\beta$  stalk region alone is capable of enhancing the coreceptor function of CD8 $\alpha$ .

*Wild-type CD8 $\beta$  restores the Ag sensitivity of a functionally inactive CD8 $\alpha$  mutant, Arg8Ala*

The x-ray structure of the H-2K<sup>b</sup>/mCD8 $\alpha\alpha$  or HLA-A2/hCD8 $\alpha\alpha$  complex revealed that Arg<sup>8</sup> (R8) of murine CD8 $\alpha$  or Arg<sup>4</sup> (R4) of human CD8 $\alpha$  forms multiple hydrogen bonds and salt bridges with the  $\beta_2$ -microglobulin ( $\beta_2$ M) (38, 39). To verify that these interactions between Arg<sup>8</sup> and  $\beta_2$ M are functionally relevant, we generated a murine CD8 $\alpha$  carrying an alanine residue in this position (CD8 $\alpha^{R8A}$ ) and tested for its coreceptor function in the N15 T cell hybridoma. Fig. 2A, upper panel, shows that the N15 cells expressing CD8 $\alpha^{R8A}$  require  $\sim$ 1000-fold higher concentrations of peptide Ag to induce a level of IL-2 production similar to that of wild-type CD8 $\alpha$ -expressing cells, indicating that the Arg<sup>8</sup>- $\beta_2$ M interaction is important for the coreceptor function of CD8 $\alpha\alpha$  homodimers. Interestingly, coexpression of CD8 $\beta$  rescues the coreceptor function of CD8 $\alpha^{R8A}$  (Fig. 2A, lower panel). This result suggests that the interaction between Arg<sup>8</sup> located within the Ig-like domain of CD8 $\alpha$  and  $\beta_2$ M is not required for the coreceptor function of CD8 $\alpha\beta$  heterodimers.

*Stalk region of CD8 $\beta$  restores the Ag sensitivity of a functionally defective CD8 $\alpha^{R8A}$  Ig-like domain*

The results in Fig. 2A raise the question of whether the Ig-like domain and/or the stalk region of CD8 $\beta$  are responsible for restoring the function of CD8 $\alpha^{R8A}$ . The availability of the chimeric CD8 $\alpha$  allows us to test whether the stalk region of CD8 $\beta$  plays a role in the function of this CD8 $\alpha^{R8A}$  mutant. We introduced the Arg8Ala mutation into the chimeric CD8 $\alpha$  to generate the chimeric CD8 $\alpha^{R8A}$ . Cells expressing the wild-type CD8 $\alpha$ , the chimeric CD8 $\alpha$ , the chimeric CD8 $\alpha^{R8A}$ , or the wild-type CD8 $\alpha\beta$  were compared for their sensitivities to peptide Ag. To eliminate

the possibility that the difference in IL-2 production is due to a difference in the expression of TCR and/or CD8 proteins, cells were analyzed by FACS for surface expression of these proteins. Fig. 2B shows that the N15TCR expression is quite comparable in these cell lines, as monitored by the V $\beta$ 5-specific Ab, MR9.4. Expression levels of CD8 $\alpha$  on these cell lines were evaluated by staining with five anti-CD8 $\alpha$  Abs: 53.6.72, 19/178, H59, YTS105, and YTS169. Fig. 2B shows that the staining patterns of all Abs, except H59, are very similar, indicating comparable expression levels of CD8 $\alpha$  proteins. H59 detects the wild-type CD8 $\alpha$ , but not the CD8 $\alpha^{R8A}$  mutant or the chimeric CD8 $\alpha^{R8A}$ . It appears that Arg<sup>8</sup> is part of the epitope for H59 Ab. Thus differential staining detected by H59 and other Abs also allow us to verify the identity of the CD8 $\alpha^{R8A}$  variant. Importantly, since chimeric CD8 $\alpha^{R8A}$  retains antigenic epitopes of all four anti-CD8 $\alpha$  Abs, it appears that the introduction of the CD8 $\beta$  stalk region did not alter the overall structure of the Ig-like domain of the chimeric CD8 $\alpha$  protein.

The functional impact of the replaced  $\beta$  stalk in the context of CD8 $\alpha^{R8A}$  was evaluated by IL-2 production triggered by peptide Ag. Fig. 2C shows that, to our surprise, the N15 cells expressing chimeric CD8 $\alpha^{R8A}$  are  $\sim$ 1000-fold more sensitive to peptide Ag than those expressing CD8 $\alpha^{R8A}$  with the  $\alpha$  stalk. The peptide Ag sensitivity of chimeric CD8 $\alpha^{R8A}$ -expressing N15 cells is actually comparable to that observed in cells expressing either chimeric CD8 $\alpha\alpha$  homodimers or wild-type CD8 $\alpha\beta$  heterodimers (Fig. 2C). Thus, not only can the functional defect caused by the Arg8Ala mutation in the CD8 $\alpha$  Ig-like domain be fully rescued by the replacement of the  $\beta$  stalk region, but it can also enhance sensitivity to a level similar to that of CD8 $\alpha\beta$  wild type. These results suggest that the introduction of the CD8 $\beta$  stalk region enhanced the coreceptor function of CD8 $\alpha$ , presumably by altering the interaction

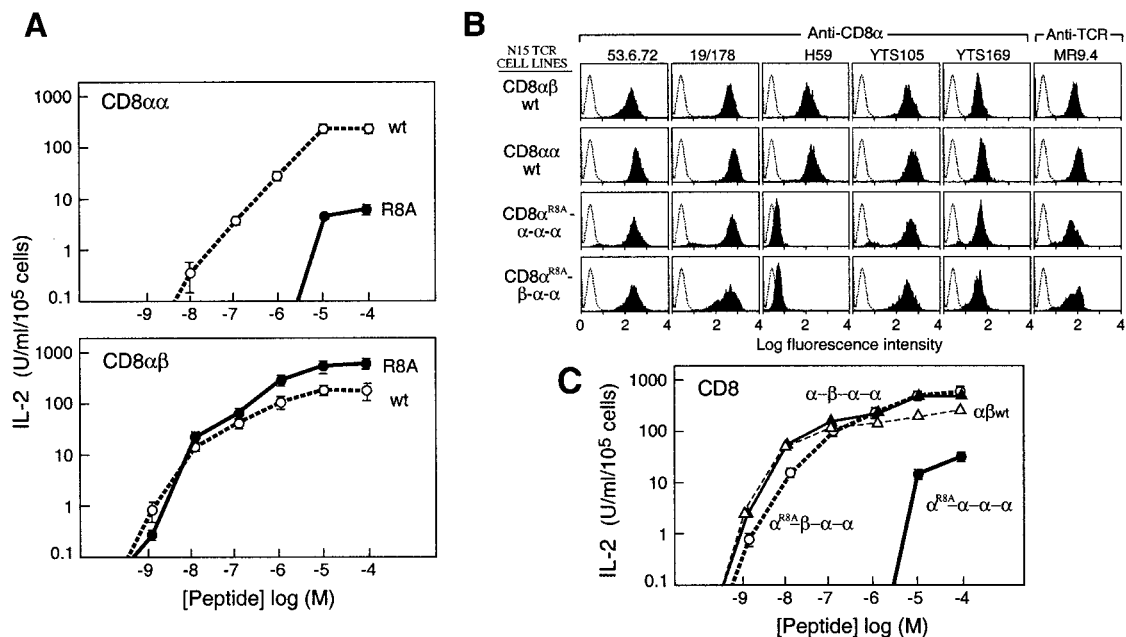


**FIGURE 2.** The  $\beta$  stalk region restores the Ag sensitivity of a functionally defective mutant, CD8 $\alpha^{R8A}$ . A, R8 residue of CD8 $\alpha$ 1 subunit is critical for coreceptor function of CD8 $\alpha\alpha$ , but not CD8 $\alpha\beta$ . Upper panel, IL-2 production curves of cell lines expressing wild-type CD8 $\alpha\alpha$  and CD8 $\alpha^{R8A}$   $\alpha$ - $\alpha$ - $\alpha$ . Lower panel, IL-2 production curves of the wild-type CD8 $\alpha\beta$  and CD8 $\alpha^{R8A}$   $\beta$ . Units of IL-2 production include the mean  $\pm$  SD of triplicate samples. B, FACS analysis of the CD8 $\alpha$  and chimeric CD8 $\alpha$  N15 T cell transfectants. The surface expression of TCR and CD8 $\alpha$  epitopes on the transfectants was detected by indirect fluorescence staining as described previously. The cells express a comparable level of TCR and CD8 $\alpha$  molecules. The R8A mutation abolishes H59 Ab binding. C, IL-2 production curves of transfectants expressing chimeric CD8 variants. IL-2 production curves are represented with a filled circle for CD8 $\alpha^{R8A}$   $\alpha$ - $\alpha$ - $\alpha$ , an open circle for chimeric CD8 $\alpha^{R8A}$   $\beta$ - $\alpha$ - $\alpha$ , a filled triangle for chimeric CD8 $\alpha^{R8A}$   $\alpha$ - $\beta$ - $\alpha$ - $\alpha$ , and an open triangle for CD8 $\alpha\beta$ -wt. IL-2 production was detected at  $10^{-9}$  M VSV8 peptide in the cell line CD8 $\alpha^{R8A}$   $\beta$ - $\alpha$ - $\alpha$ , which is a 1000-fold decrease, in terms of the amount of peptide concentration required, relative to the CD8 $\alpha^{R8A}$   $\alpha$ - $\alpha$ - $\alpha$  mutant.

with MHCI such that the Arg<sup>8</sup>- $\beta_2$ M interaction is no longer required for the coreceptor function. Importantly, these results extend our previous observation and show that, without formally eliminating the role of the Ig-like domain of the CD8 $\beta$ , the stalk region of CD8 $\beta$  is sufficient for rescuing the functional defect in CD8 $\alpha^{R8A}$ .

*MHCI employs similar structural determinants to interact with CD8 $\alpha$  and chimeric CD8 $\alpha^{R8A}$*

Since the CD8 $\alpha$ Arg<sup>8</sup>- $\beta_2$ M interaction is no longer needed for coreceptor function of the chimeric CD8 $\alpha$  homodimer, we questioned whether MHCI employs different structural determinants to interact with the chimeric CD8 $\alpha$ . To address this, we mutated three key residues (Lys<sup>198</sup> on the AB loop, Gln<sup>226</sup> and Asp<sup>227</sup> on the CD loop) in the  $\alpha 3$  domain of H-2K<sup>b</sup> which, based on the crystal structure of CD8 $\alpha$ /K<sup>b</sup> complex (Fig. 3A), form hydrogen bonds with wild-type CD8 $\alpha$  (39). We reasoned that if the Ig-like domains of wild-type CD8 $\alpha$  and chimeric CD8 $\alpha^{R8A}$  are oriented differently, their interactions with the  $\alpha 3$  domain of H-2K<sup>b</sup> are likely to be different. It is conceivable that a change(s) in the CD8 $\alpha$ -H-2K<sup>b</sup> interaction will affect the efficiency of peptide Ag presentation and, hence, IL-2 production. APCs expressing each of these H-2K<sup>b</sup> mutants were generated and used to present VSV8 peptide in the IL-2 production assay. Fig. 3B, upper panel, shows the response of N15 cells expressing wild-type CD8 $\alpha$  to peptide Ag presented by wild-type or mutant H-2K<sup>b</sup>. APC expressing Gln226Ala H-2K<sup>b</sup> are ~10 times less efficient than APC expressing wild-type H-2K<sup>b</sup>, and APC expressing Asp227Ala H-2K<sup>b</sup> exhibit activity similar to APC expressing wild-type H-2K<sup>b</sup>. Interestingly, APC expressing Lys198Ala H-2K<sup>b</sup> exhibit a subtle change in Ag presentation; at lower concentrations of peptide Ag they are more efficient, but at higher concentrations they are less efficient, than the APC-expressing, wild-type H-2K<sup>b</sup>. Most importantly, very similar profiles were observed when APC cells expressing each of these three MHCI variants were used to present peptide Ag to N15 cells expressing chimeric CD8 $\alpha^{R8A}$  (Fig. 3B, middle panel), including the unique profile observed in the APC expressing Lys198Ala H-2K<sup>b</sup> (a characteristic crossing over between K<sup>b</sup>-wild type (wt) and K<sup>b</sup> Lys198Ala). Besides the similar profile of dose-response curves, the Ag sensitivity of chimeric CD8 $\alpha^{R8A}$  is enhanced by ~10- to 40-fold when stimulated by APC expressing wild-type K<sup>b</sup> or by Lys198Ala or Asp227Ala K<sup>b</sup> variants compared with that of CD8 $\alpha$ -expressing cells (Fig. 3B, middle panel). When wild-type CD8 $\alpha\beta$  transfectants were stimulated with these APCs expressing K<sup>b</sup> variants, similar profiles of IL-2 production curves were observed, except that greater amounts of IL-2 were produced and higher sensitivities of Ag recognition were observed at peptide concentrations  $<10^{-6}$  M (Fig. 3B, lower panel). These observations are in agreement with our findings that the  $\beta$  subunit, or  $\beta$  stalk region, enhances the coreceptor function of CD8. Mutations at residues where MHCI contacts the CD8 Ig-like domain have a similar impact on the coreceptor function of all three cells, wild type CD8 $\alpha$ , chimeric CD8 $\alpha^{R8A}$ , and CD8 $\alpha\beta$ -wt. These results strongly suggest that the H-2K<sup>b</sup> employs similar structural determinants for its interactions with these CD8 $\alpha$  variants.

*Introduction of CD8 $\beta$  stalk compromises the blocking activity of an anti-CD8 $\alpha$  Ab*

Since the CD8 $\alpha$  Arg<sup>8</sup>- $\beta_2$ M interaction is not required for the coreceptor function of chimeric CD8 $\alpha$ , but structural determinants of MHCI employed to interact with the Ig-like domain of CD8 $\alpha$  and chimeric CD8 $\alpha$  remained the same, we questioned whether introduction of the  $\beta$  stalk leads to a topological alteration in the complex of  $\beta_2$ M and the Ig-like domain of chimeric CD8 $\alpha$ . To inves-

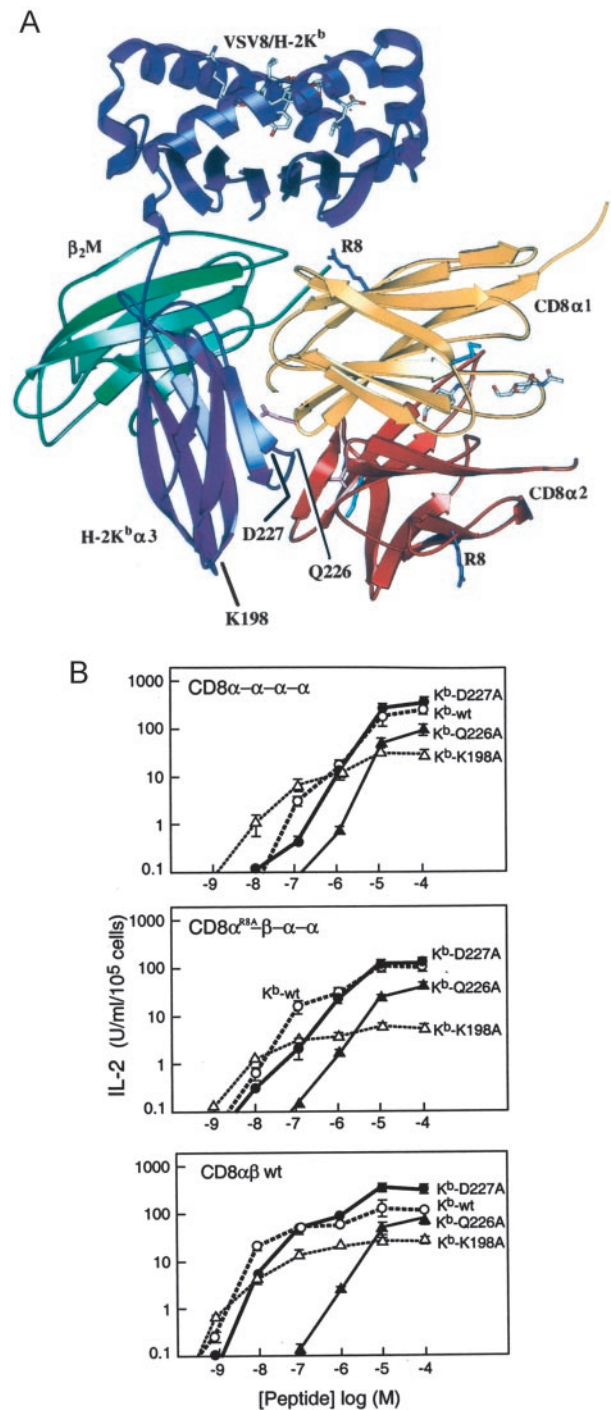


**FIGURE 3.** Chimeric CD8 $\alpha^{R8A}$  contacts the same key K<sup>b</sup> residues to mediate coreceptor function as CD8 $\alpha\alpha$ -wt. *A*, The crystal structure-based model of mCD8 $\alpha\alpha$ /H-2K<sup>b</sup>. The mCD8 $\alpha\alpha$ /H-2K<sup>b</sup> is a RASTER three-dimensional-rendered MOLSCRIPT drawing (47, 48). In the figure the K<sup>b</sup> heavy chain is in blue,  $\beta_2$ M is in green, CD8 $\alpha 1$  is in yellow, and CD8 $\alpha 2$  is in red. The side chains of the R8 residue on both subunits of CD8 $\alpha$  are labeled, and the positions of K198, Q226, and D227 in the K<sup>b</sup> molecule are indicated. *B*, IL-2 production curves of transfectant expressing wild-type CD8 $\alpha\alpha$  (upper panel), chimeric CD8 $\alpha^{R8A}$  (middle panel), and wild-type CD8 $\alpha\beta$  (lower panel) that were stimulated with mutant APC loaded with the indicated amounts of VSV8.

tigate such a possibility, we analyzed the inhibitory effects of a series of anti-CD8 $\alpha$  Abs that were used previously for the evaluation of surface expression of CD8 $\alpha$  (Fig. 2B). Each of these Abs

recognizes an epitope within the Ig-like domain, and several of them are capable of blocking the coreceptor function of CD8 $\alpha\alpha$  and CD8 $\alpha\beta$  (data not shown). We reasoned that if the overall topology of the CD8 $\alpha$ -MHCI complexes were altered due to introduction of the  $\beta$  stalk, the inhibitory activity of one or more of these blocking Abs might be compromised. As shown in Fig. 4A, upper panel, in cells expressing wild-type CD8 $\alpha$  homodimer, anti-CD8 $\alpha$  mAbs 53.6.72 and YTS169 completely block IL-2 production within a comparable range. However, in the cell line expressing chimeric CD8 $\alpha^{\text{RSA}}$  homodimer (Fig. 4A, lower panel), the anti-CD8 $\alpha$  mAb 53.6.72 blocks IL-2 production completely, but Ab YTS169 blocks IL-2 production 10- to 100-fold less effectively. Furthermore, this result is similar to the Ab blocking experiment performed on the cells expressing CD8 $\alpha\beta$ -wt heterodimer (Fig. 4B). Since the differential sensitivity to the YTS169 Ab blocking is not due to any difference in the expression levels of these CD8 $\alpha$  variants (Fig. 2B, anti-CD8 $\alpha$  staining) or TCR (Fig. 2B, anti-TCR staining), nor is it due to a loss of the antigenic epitope of Ab YTS169 in chimeric CD8 $\alpha^{\text{RSA}}$  (Fig. 2B, YTS169 staining), we hypothesized that the less bulky Fab of YTS169 should have more profound differential effects in blocking these two cell lines. Based on the results of these experiments, as shown in Fig. 4A, the Fab of YTS169 is 100 times more effective in blocking the coreceptor function of wild-type CD8 $\alpha$  than chimeric CD8 $\alpha^{\text{RSA}}$ . Since the antigenic epitope is present in the Ig-like domain of CD8 $\alpha$  (36), the lesser effectiveness of YTS169 Ab in blocking IL-2 production on chimeric CD8 $\alpha$ -expressing cells suggests that the introduction of the  $\beta$  stalk leads to a change in the interaction between the Ig-like domain of CD8 $\alpha$  and MHCI, such that the binding of YTS169 is better tolerated with respect to the coreceptor function.

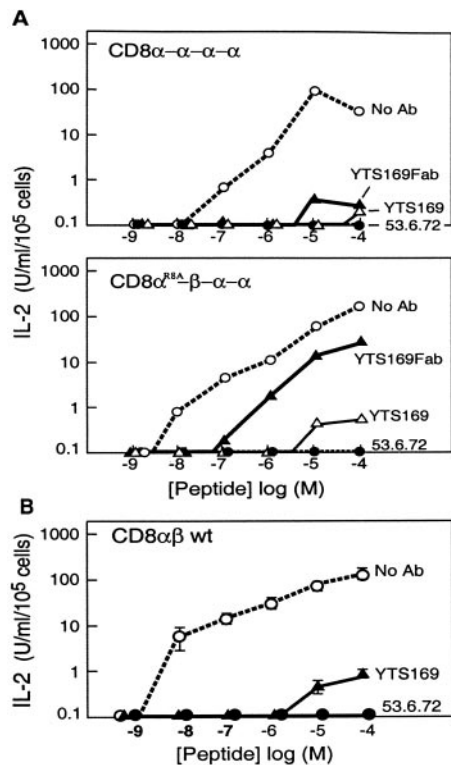


**FIGURE 4.** Anti-CD8 $\alpha$  Abs block the chimeric CD8 $\alpha^{\text{RSA}}$  homodimer differently. *A*, IL-2 production curves of cell lines expressing homodimer wild-type CD8 $\alpha\alpha$  (upper panel) or chimeric CD8 $\alpha^{\text{RSA}}$  (lower panel) in the presence or the absence of anti-CD8 $\alpha$  mAbs or Fab. *B*, IL-2 production curves of cell lines expressing heterodimer CD8 $\alpha\beta$ -wt in the presence or the absence of the blocking Abs.

This is consistent with the observation that Arg8Ala is not critical for CD8 $\alpha\beta$  coreceptor function. These results indicated that introduction of the  $\beta$  stalk does not affect the overall structure of the CD8 $\alpha$  Ig-like domain, but does alter the topology of the CD8 $\alpha$ -MHCI complex.

#### Chimeric CD8 $\alpha^{\text{RSA}}$ retains the glycosylation patterns of the CD8 $\beta$ subunit

The stalk regions of CD8 $\alpha$  and CD8 $\beta$  exhibit different glycosylation patterns. The *O*-linked glycosylation of CD8 $\beta$  is regulated upon differentiation or activation, suggesting that these carbohydrates may play a role in the function of CD8 $\beta$ . We therefore investigated whether the characteristic glycosylation pattern of CD8 $\beta$  is retained in the chimeric CD8 $\alpha$ . We showed that surface-expressed CD8 $\beta$  migrates as a set of bands with apparent molecular mass ranging from 30–36 kDa on SDS-PAGE (Fig. 5, lanes 2 and 5), and CD8 $\alpha$  migrates as a more discrete band with an apparent molecular mass of  $\sim$ 42 kDa (Fig. 5, lanes 1 and 2). These patterns are consistent with previous reports, which showed that the glycosylation on CD8 $\alpha$  and CD8 $\beta$  is significantly different (20, 32). The cell surface-expressed chimeric CD8 $\alpha^{\text{RSA}}$  migrates as a series of bands similar to those of CD8 $\beta$  proteins observed in the CD8 $\alpha\beta$  complexes (Fig. 5, lane 4 vs lane 2). Thus, the replaced  $\beta$  stalk lowers the apparent overall molecular mass of chimeric

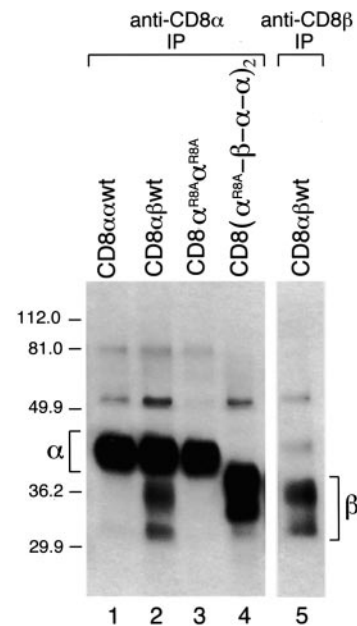


**FIGURE 5.** SDS-PAGE analysis of surface CD8 $\alpha$  and chimeric CD8 $\alpha^{\text{RSA}}$  on T cell transfectants. After surface biotinylation, the CD8 $\alpha$  or CD8 $\beta$  subunits were immunoprecipitated from the designated cell lines using mAb 53.6.72 for CD8 $\alpha$  or YTS 156 for CD8 $\beta$ . The immunoprecipitates were run on 12.5% SDS-PAGE gels under reducing conditions and blotted onto nitrocellulose membranes, and proteins were detected with ECL. The  $\alpha$  subunits of the wild-type homodimer CD8 $\alpha\alpha$  and CD8 $\alpha^{\text{RSA}}\alpha^{\text{RSA}}$  were run at 40 kDa as indicated (lanes 1 and 3). Anti-CD8 $\alpha$  Ab immunoprecipitated both CD8 $\alpha$  and CD8 $\beta$  from transfectants expressing CD8 $\alpha\beta$  (lane 2). Under reducing conditions,  $\alpha$  and  $\beta$  subunits migrate at 40 and 30–36 kDa, respectively. The heterogeneous migration of the CD8 $\beta$  subunit is due to variable glycosylation at *O*-linked sites on the  $\beta$  stalk region. The same result is observed on the anti-CD8 $\beta$  IP (lane 5). In lane 4, the immunoprecipitation of surface chimeric CD8 $\alpha^{\text{RSA}}\beta$ - $\alpha$ - $\alpha$  molecules using the anti-CD8 $\alpha$  mAb reveals at least two major bands and one minor band with a molecular mass range of 32–38 kDa. This result indicates that the chimeric CD8 $\alpha^{\text{RSA}}$  coreceptor shows the heterogeneous mobility of the wild-type  $\beta$  stalk region in SDS-PAGE.

CD8 $\alpha^{R8A}$ . Importantly, the broad range of its apparent molecular mass suggests that the  $\beta$  stalk retains its glycosylation patterns in the chimeric CD8 $\alpha^{R8A}$ . Similar heterogeneous bands are observed on the surface of cells expressing chimeric CD8 $\alpha$  (data not shown). These results indicate that the chimeric CD8 $\alpha^{R8A}$  is glycosylated similarly to the wild-type CD8 $\beta$ .

## Discussion

In the search for the structural element in CD8 $\beta$ -chain that is responsible for the better coreceptor function of CD8 $\alpha\beta$ , we compared CD8 $\alpha$  and CD8 $\beta$  and found that the stalk regions of these two subunits are quite different in primary sequence, physical length, and general glycosylation patterns. These distinctions prompted us to investigate the role of the  $\beta$  stalk region in the coreceptor function of CD8. Our results showed that with the replaced  $\beta$  stalk region, the chimeric CD8 $\alpha$  dimer exhibits CD8 $\alpha\beta$  heterodimer-like coreceptor efficiency. The observation that the coreceptor function of CD8 $\alpha$  can be enhanced by introduction of the  $\beta$  stalk region was unexpected. This led us to search for potential structural alterations in the Ig-like domain of chimeric CD8 $\alpha$  that might be brought about by the introduction of the  $\beta$  stalk. Since comparable staining of four anti-CD8 $\alpha$  Ig-like domain Abs was observed in chimeric CD8 $\alpha\alpha$ - and CD8 $\alpha\beta$ -expressing cells, it appears that no major structural alteration results from the introduction of the  $\beta$  stalk region. We reasoned that if the CD8 $\alpha$  stalk region and CD8 $\beta$  stalk region “present” the Ig-like domain of CD8 $\alpha$  differently, then the corresponding Ig-like domain contact residues on the MHCI are likely to be different. Yet, while the Ag titration profiles obtained from the three H-2K<sup>b</sup> variants are quite different, the titration profiles obtained from wild-type CD8 $\alpha$ - and chimeric CD8 $\alpha$ -expressing cells in response to each H-2K<sup>b</sup> variant are virtually identical. Thus, the stalk region of CD8 $\beta$  is capable of modulating the coreceptor function of chimeric CD8 $\alpha$  without altering the apparent structure of the adjacent Ig-like domain or causing the MHCI to use different residues to interact with the Ig-like domain.

Most importantly, we found that binding of YTS169 or its Fab to the Ig-like domain has less inhibitory effect on the coreceptor function of chimeric CD8 $\alpha$  or CD8 $\alpha\beta$ -wt than on that of CD8 $\alpha$ -wt. This is despite the fact that YTS169 binds to all three types of CD8 molecules. Thus, the inability of YTS169 to block the coreceptor function of chimeric CD8 $\alpha^{R8A}$  is not due to the loss of its antigenic epitope on these proteins. The fact that chimeric CD8 $\alpha$  and wild-type CD8 $\alpha$  (in the context of CD8 $\alpha\alpha$  homodimer and CD8 $\alpha\beta$  heterodimer) share the antigenic epitopes of all five mAbs indicates they share a similar overall structural conformation. Together with the fact that K<sup>b</sup> is employing the similar structural determinants for its interaction with chimeric CD8 $\alpha$  and wild-type CD8, we reasoned that the complexes of chimeric CD8 $\alpha^{R8A}$  and K<sup>b</sup> and wild-type CD8 $\alpha$  and K<sup>b</sup> must be topologically so different such that the former, but not the latter, is capable of accommodating the occupancy of YTS169. Thus, the introduction of the  $\beta$  stalk region leads to a change in the overall topology of the CD8 $\alpha$ /MHCI complexes. This is consistent with our own observation, which showed that the CD8 $\alpha$  Arg<sup>8</sup> (this report), Glu<sup>27</sup> or Asn<sup>107</sup> (X. Wang, K. Tang, Y. Le, T. Witte, J. Wong, and H. C. Chang, unpublished observations) are not essential for the coreceptor function in the context of the CD8 $\alpha\beta$  heterodimer. It seems plausible that CD8 $\alpha$  is capable of employing at least two sets of residues to interact with the classical MHCI molecule in the context of the CD8 $\alpha\alpha$  homodimer vs CD8 $\alpha\beta$  heterodimer. Indeed, this idea is further supported by a recent study that reported that critical residues in CD8 $\alpha\alpha$  have a different impact on tetramer binding of H-2K<sup>b</sup> vs TL, thymic leukemia Ag (40).

It should be noted that a previous report (41) showed the coexpression of human CD8 $\alpha$  Arg4Lys mutant (the counterpart of Arg8Ala in mouse CD8 $\alpha$ ) with human CD8 $\beta$  in COS-7 cells com-

pletely abolishes the adhesion capacity of human CD8 $\alpha^{R4K}\beta$  to HLA-A2-expressing cells. These observations led to the conclusion that wild-type CD8 $\beta$  subunits are not able to rescue the adhesion function of the defective CD8 $\alpha^{R4K}$ . The reason why Arg<sup>4</sup> is required in the context of human CD8 $\alpha\beta$  is not clear. It is conceivable that one or more differences in the origin of CD8 (mouse vs human), the expression systems (established cell line vs transient expression system), the assay methods (IL-2 production vs cell-cell adhesion), and the nature of the mutation (Arg to Ala vs Arg to Lys) may account for such a discrepancy. Additional investigations will be needed to resolve this inconsistency.

The idea that residues on H-2K<sup>b</sup> involved in the interaction with CD8 $\alpha\beta$  or chimeric CD8 $\alpha$  appear to be similar is based on the analysis of IL-2 production triggered by APCs expressing H-2K<sup>b</sup> variants, differing in one key residue involved in direct contact with CD8 $\alpha$ . Both mutagenesis and crystallographic data indicated that the  $\alpha$ 3 CD loop of the MHCI molecule (residues 220–228) is key for the interaction with the CDR-like loops of CD8 $\alpha$  (2, 3, 38, 39). Specifically, the side chain of Gln<sup>226</sup> extends between two of the CDR-like loops and forms hydrogen bonds with Ser<sup>108</sup> in the  $\alpha$ 1 subunit and Ser<sup>27</sup> in the  $\alpha$ 2 subunit of CD8 $\alpha$  (39). This structural information is consistent with our observation that the Gln<sup>226</sup>Ala mutation compromises IL-2 production. In addition, the crystal structure revealed that the AB loop of H-2K<sup>b</sup> is pointing toward the CDR2-like domain of CD8 $\alpha$  and is stabilized by hydrogen bonds between Lys<sup>198</sup> of H-2K<sup>b</sup> and Ser<sup>59</sup> of CD8 $\alpha$ 2 as well as Glu<sup>196</sup> of H-2K<sup>b</sup> and Asn<sup>61</sup> of CD8 $\alpha$ 2 (39). Even though the effect of the Lys198Ala mutation is not drastic, it leads to a characteristic profile of IL-2 production. We were, however, surprised by the observation that the Asp227A mutation on H-2K<sup>b</sup> has little impact on these CD8 variants. Prior studies on the H-2K<sup>b</sup> or D<sup>b</sup> molecules showed that mutation of Asp227Lys or Glu227Lys abrogates the Ag recognition by CD8-dependent CTL (4, 42, 43). It is possible that the Asp227Lys and Glu227Lys mutations each introduce a bulky positively charged side chain, which may have caused an additional structural perturbation(s) that did not occur in the Asp227Ala mutation.

Besides the distinct polypeptide backbones and the different physical lengths, the stalk regions of CD8 $\alpha$  and CD8 $\beta$  also drastically differ from each other in their glycosylation patterns. The glycan adducts associated with these regions can conceivably govern their ability to orient the Ig-like domain and ultimately lead to a differential efficiency in coreceptor function. In fact, it was shown that the oligosaccharides proximal to the transmembrane region tend to be evolutionarily conserved and appeared to be able to restrict the orientation of certain cell adhesion molecules (33). Similarly, it was proposed that lacking *N*-linked carbohydrates might directly enhance the TCR clustering and lead to a lower threshold for T cell activation (44). These observations are consistent with our working model, in that additional carbohydrates on the stalk of the CD8 $\alpha$ -chain may effectively restrict the possible orientations of the adjacent Ig-like domains and interaction with the MHCI-peptide Ag complexes and may ultimately lead to a lower efficiency in Ag presentation.

It appears that even though mouse CD8 $\beta$  is capable of forming dimers intracellularly, its expression on the cell surface requires association with CD8 $\alpha$  and presentation as a heterodimer. It has been our ongoing interest to search for the structural element(s) that prevents the surface maturation of the CD8 $\beta$ -chain. While this is not directly related to the current study reported here, we should mention that our results show that the introduction of  $\beta$  stalk did not affect the ability of the chimeric CD8 $\alpha$  to express on the cell surface, indicating that the  $\beta$  stalk region is not responsible for the inability of CD8 $\beta$  to be expressed on the cell surface. Together

with the observation that deletion of the  $\beta$ -chain cytoplasmic domain did not rescue the surface expression of CD8 $\beta$ , it appears that the mouse  $\beta$ -chain Ig-like domain may play a critical role in the intracellular retention of CD8 $\beta$ . Additional experiments using chimeric proteins containing the  $\beta$ -chain Ig-like domain in the context of CD8 $\alpha$  should help to verify such a possibility.

In summary, our observation implicates that the stalk regions of CD8 $\alpha$  and CD8 $\beta$  are capable of delivering the Ig-like domain of either CD8 $\alpha$  or  $\beta$  to interact with the MHCI molecule. The shorter length and regulated glycosylation modifications and glycan moieties in the CD8 $\beta$  stalk make CD8 $\alpha\beta$  a more effective coreceptor even at low peptide Ag concentrations, while CD8 $\alpha\alpha$  is only functional in the presence of a high abundance of peptide Ag.

## Acknowledgments

We are grateful to Dr. E. Reinherz for his total support that made this study possible. We thank Drs. Linda Clayton and Yen-Ming Hsu for their critical reading of and insightful suggestions about the manuscript.

## References

- Bonneville, M., and F. Lang. 2002. CD8: from coreceptor to comodulator. *Nat. Immunol.* 1:12.
- Salter, R. D., A. M. Norment, B. P. Chen, C. Clayberger, A. M. Krensky, D. R. Littman, and P. Parham. 1989. Polymorphism in the  $\alpha 3$  domain of HLA-A molecules affects binding to CD8. *Nature* 338:345.
- Salter, R. D., R. J. Benjamin, P. K. Wesley, S. E. Buxton, T. P. J. Garrett, C. Clayberger, A. M. Krensky, A. M. Norment, D. R. Littman, and P. Parham. 1990. A binding site for the T-cell co-receptor CD8 on the  $\alpha 3$  domain of HLA-A2. *Nature* 345:41.
- Luescher, I. F., E. Vivier, A. Layer, J. Mahiou, F. Godeau, B. Malissen, and P. Romero. 1995. CD8 modulation of T-cell antigen receptor-ligand interactions on living cytotoxic T lymphocytes. *Nature* 373:353.
- Cantor, H., and E. A. Boyse. 1975. Functional subclasses of T-lymphocytes bearing different Ly antigens: the generation of functionally distinct T-cell subclasses is a differentiative process independent of antigen. *J. Exp. Med.* 141:1376.
- Daniels, M. A., and S. C. Jameson. 2000. Critical role for CD8 in T cell receptor binding and activation by peptide/major histocompatibility complex multimers. *J. Exp. Med.* 191:335.
- Miceli, M. C., and J. R. Parnes. 1993. Role of CD4 and CD8 in T cell activation and differentiation. *Adv. Immunol.* 53:59.
- Reinherz, E. L., and S. F. Schlossman. 1980. The differentiation and function of human T lymphocytes. *Cell* 19:821.
- Moebius, U., G. Kober, M. L. Griscelli, T. Hercend, and S. C. Meuer. 1991. Expression of different CD8 isoforms on distinct human lymphocyte subpopulations. *Eur. J. Immunol.* 21:1793.
- Terry, L. A., J. P. DiSanto, T. N. Small, and N. Flomenberg. 1990. Differential expression and regulation of the human CD8 $\alpha$  and CD8 $\beta$  chains. *Tissue Antigen* 35:82.
- de Toter, D., P. L. Tazzari, J. P. DiSanto, P. F. di Celle, D. Raspadori, R. Conte, M. Gobbi, G. B. Ferrara, N. Flomenberg, and F. Lauria. 1992. Heterogeneous immunophenotype of granular lymphocyte expansions: differential expression of the CD8 $\alpha$  and CD8 $\beta$  chains. *Blood* 80:1765.
- DiSanto, J. P., R. W. Knowles, and N. Flomenberg. 1988. The human Lyt-3 molecule requires CD8 for cell surface expression. *EMBO J.* 7:3465.
- Gorman, S. D., Y. H. Sun, R. Zamoyska, and J. R. Parnes. 1988. Molecular linkage of the Ly-3 and Ly-2 genes: requirement of Ly-2 for Ly-3 surface expression. *J. Immunol.* 140:3646.
- Norment, A. M., and D. R. Littman. 1988. A second subunit of CD8 is expressed in human T cells. *EMBO J.* 7:3433.
- Panaccio, M., M. T. Gillespie, I. D. Walker, L. Kirszbaum, J. A. Sharpe, G. H. Tobias, I. F. C. McKenzie, and N. J. Deacon. 1987. Molecular characterization of the murine cytotoxic T-cell membrane glycoprotein Ly-3 (CD8). *Proc. Natl. Acad. Sci. USA* 84:6874.
- Shiue, L., S. D. Gorman, and J. R. Parnes. 1988. A second chain of human CD8 is expressed on peripheral blood lymphocytes. *J. Exp. Med.* 168:1993.
- Torres-Nagel, N., E. Kraus, M. H. Brown, G. Tiefenthaler, R. Mitnacht, A. F. Williams, and T. Hunig. 1992. Differential thymus dependence of rat CD8 isoform expression. *Eur. J. Immunol.* 22:2841.
- Gapin, L., H. Cheroutre, and M. Kronenberg. 1999. Cutting edge: TCR $\alpha\beta^+$  CD8 $\alpha\alpha^+$  T cells are found in intestinal intraepithelial lymphocytes of mice that lack classical MHC class I molecules. *J. Immunol.* 163:4100.
- Hayday, A., E. Theodoridis, E. Ramsburg, and J. Shires. 2001. Intraepithelial lymphocytes: exploring the third way in immunology. *Nat. Immunol.* 2:997.
- Witte, T., R. Spoerl, and H. C. Chang. 1999. The CD8 $\beta$  ectodomain contributes to the augmented coreceptor function of CD8 $\alpha\beta$  heterodimers relative to CD8 $\alpha\alpha$  homodimers. *Cell. Immunol.* 191:90.
- Renard, V., P. Romero, E. Vivier, B. Malissen, and I. F. Luescher. 1996. CD8 $\beta$  increases CD8 coreceptor function and participation in TCR-ligand binding. *J. Exp. Med.* 184:2439.
- Irie, H. Y., M. S. Mong, A. Itano, M. E. Crooks, D. R. Littman, S. J. Burakoff, and E. Robey. 1998. The cytoplasmic domain of CD8 $\beta$  regulates Lck kinase activation and CD8 T cell development. *J. Immunol.* 161:183.
- Arcaro, A., C. Gregoire, T. R. Bakker, L. Baldi, M. Jordan, L. Goffin, N. Boucheron, F. Wurm, P. A. van der Merwe, B. Malissen, et al. 2001. CD8 $\beta$  endows CD8 with efficient coreceptor function by coupling T cell receptor/CD3 to raft-associated CD8/p56<sup>lck</sup> complexes. *J. Exp. Med.* 194:1485.
- Wheeler, C. J., Y. F. Chen, T. A. Potter, and J. R. Parnes. 1998. Mechanisms of CD8 $\beta$ -mediated T cell response enhancement: interaction with MHC class I $\beta_2$ -microglobulin and functional coupling to TCR/CD3. *J. Immunol.* 160:4199.
- Wheeler, C. J., P. Hoegen von, and J. R. Parnes. 1992. An immunological role for the CD8  $\beta$ -chain. *Nature* 357:247.
- Bosselut, R., L. Feigenbaum, S. O. Sharrow, and A. Singer. 2001. Strength of signaling by CD4 and CD8 coreceptor tails determines the number but not the lineage direction of positively selected thymocytes. *Immunity* 14:483.
- Moody, A. M., D. Chui, P. A. Reche, J. J. Priatel, J. D. Marth, and E. L. Reinherz. 2001. Developmentally regulated glycosylation of the CD8 $\alpha\beta$  coreceptor stalk modulates ligand binding. *Cell* 107:501.
- Zamoyska, R. 1994. The CD8 coreceptor revisited: one chain good, two chains better. *Immunity* 1:243.
- Wu, W., P. H. Harley, J. A. Punt, S. O. Sharrow, and K. P. Kearse. 1996. Identification of CD8 as a peanut agglutinin (PNA) receptor molecule on immature thymocytes. *J. Exp. Med.* 184:759.
- Priatel, J. J., D. Chui, N. Hiraoka, C. J. Simmons, K. B. Richardson, D. M. Page, M. Fukuda, N. M. Varki, and J. D. Marth. 2000. The ST3Gal-I sialyltransferase controls CD8<sup>+</sup> T lymphocyte homeostasis by modulating O-glycan biosynthesis. *Immunity* 12:273.
- Daniels, M. A., L. Devine, J. D. Miller, J. M. Moser, A. E. Lukacher, J. D. Altman, P. Kavathas, K. A. Hogquist, and S. C. Jameson. 2001. CD8 binding to MHC class I molecules is influenced by T cell maturation and glycosylation. *Immunity* 15:1051.
- Casabo, L. G., C. Mamalaki, D. Kioussis, and R. Zamoyska. 1994. T Cell activation results in physical modification of the mouse CD8 $\beta$  chain. *J. Immunol.* 152:397.
- Rudd, P. M., T. Elliott, P. Cresswell, I. A. Wilson, and R. A. Dwek. 2001. Glycosylation and the immune system. *Science* 291:2370.
- Rudd, P. M., M. R. Wormald, R. L. Stanfield, M. Huang, N. Mattsson, J. A. Speir, J. A. DiGennaro, J. S. Fetrow, R. A. Dwek, and I. A. Wilson. 1999. Roles for glycosylation of cell surface receptors involved in cellular immune recognition. *J. Mol. Biol.* 293:351.
- Witte, T., A. Smolyar, R. Spoerl, E. C. Goyarts, S. G. Nathenson, E. L. Reinherz, and H.-C. Chang. 1997. MHC recognition by immune receptors: differences among TCR versus antibody interactions with the VSV8/H-2K<sup>b</sup> complex. *Eur. J. Immunol.* 27:227.
- Kern, P., R. E. Hussey, R. Spoerl, E. L. Reinherz, and H. C. Chang. 1999. Expression, purification, and functional analysis of murine ectodomain fragments of CD8 $\alpha\alpha$  and CD8 $\alpha\beta$  dimers. *J. Biol. Chem.* 274:27237.
- Chang, H.-C., A. Smolyar, R. Spoerl, T. Witte, Y. Yao, E. C. Goyarts, S. G. Nathenson, and E. L. Reinherz. 1997. Topology of T cell receptor-peptide/class I MHC interaction defined by charge reversal complementation and functional analysis. *J. Mol. Biol.* 271:278.
- Gao, G. F., J. Tormo, U. C. Gerth, J. R. Wyer, A. J. McMichael, D. I. Stuart, J. I. Bell, E. Y. Jones, and B. K. Jakobsen. 1997. Crystal structure of the complex between human CD8 $\alpha\alpha$  and HLA-A2. *Nature* 387:630.
- Kern, P. S., M. K. Teng, A. Smolyar, J. H. Liu, J. Liu, R. E. Hussey, R. Spoerl, H. C. Chang, E. L. Reinherz, and J. H. Wang. 1998. Structural basis of CD8 coreceptor function revealed by crystallographic analysis of a murine CD8 $\alpha\alpha$  ectodomain fragment in complex with H-2K<sup>b</sup>. *Immunity* 9:519.
- Devine, L., L. Rogozinski, O. V. Naidenko, H. Cheroutre, and P. B. Kavathas. 2002. The complementarity-determining region-like loops of CD8 $\alpha$  interact differently with  $\beta_2$ -microglobulin of the class I molecules H-2K<sup>b</sup> and thymic leukemia antigen, while similarly with their  $\alpha 3$  domains. *J. Immunol.* 168:3881.
- Devine, L., J. Sun, M. R. Barr, and P. B. Kavathas. 1999. Orientation of the Ig domains of CD8  $\alpha\beta$  relative to MHC class I. *J. Immunol.* 162:846.
- Potter, T. A., T. V. Rajan, R. F. Dick II, and J. A. Bluestone. 1989. Substitution at residue 227 of H-2 class I molecules abrogates recognition by CD8-dependent, but not CD8-independent, cytotoxic T lymphocytes. *Nature* 337:73.
- Connolly, J. M., T. H. Hansen, A. L. Ingold, and T. A. Potter. 1990. Recognition by CD8 on cytotoxic T lymphocytes is ablated by several substitutions in the class I  $\alpha 3$  domain: CD8 and the T-cell receptor recognize the same class I molecule. *Proc. Natl. Acad. Sci. USA* 87:2137.
- Demetriou, M., M. Granovsky, S. Quaggin, and J. W. Dennis. 2001. Negative regulation of T-cell activation and autoimmunity by Mgat5 N-glycosylation. *Nature* 409:733.
- Classon, B. J., M. H. Brown, D. Garnett, C. Somoza, A. N. Barclay, A. C. Willis, and A. F. Williams. 1992. The hinge region of the CD8 $\alpha$  chain: structure, antigenicity, and utility in expression of immunoglobulin superfamily domains. *Int. Immunol.* 4:215.
- Leahy, D. J., R. Axel, and W. A. Hendrickson. 1992. Crystal structure of a soluble form of the human T cell coreceptor CD8 at 2.6 Å resolution. *Cell* 68:1145.
- Kraulis, P. J. 1991. MOLSCRIPT: a program to produce both detailed and schematic plots. *J. Appl. Crystallogr.* 24:946.
- Merritt, E., and M. E. P. Murphy. 1994. Raster3D version 2.0 version: a program for photorealistic molecular graphics. *Acta Crystallogr. D* 50:869.